ELSEVIER

BioSystems 66 (2002) 1–10

BioSystems

www.elsevier.com/locate/biosystems

Alternans and 2:1 rhythms in an ionic model of heart cells

Christian Zemlin [a,*], Eberhard Storch [b], Hanspeter Herzel [a]

[a] *Innovationskolleg Theoretische Biologie, Invalidenstr. 43, 10115 Berlin, Germany*

[b] *Johannes-Müller-Institut für Physiologie, Universitätsklinikum Charité, Humboldt-Universität zu Berlin, Tucholskystr. 2, 10117 Berlin, Germany*

Received 11 June 2001; received in revised form 18 February 2002; accepted 22 February 2002

Abstract

ECG alternans is commonly held to be an indicator of electrical instability of the heart, but the development of alternans has not yet been fully understood theoretically. We investigate the onset of alternans and 2:1 rhythms for stimulation at increasing frequencies in the Beeler–Reuter model, a simple ionic model of cardiac tissue. We find hysteresis and bistability at the onset of alternans; well-timed stimuli can switch between the two limit cycles. We determine quantitatively the effect of blocking specific ionic currents. Moreover, we find that calcium buffers generally promote alternans.

Keywords: Beeler–Reuter model; ECG alternans; Calcium buffer

1. Introduction

Nonlinear dynamics have been used successfully to understand biological rhythms (see Winfree, 1987; Glass and Mackey, 1988; Goldbeter, 1996, for nonlinear dynamics in the heart in particular, see Glass et al., 1991; Panfilov and Holden, 1997). A common rhythm in biological signals is *alternans*, in which a signal consists of two alternating segments. Alternans often develop out of a periodic signal when a parameter is changed; it is then an example of a period doubling bifurcation.

Mechanical alternans in the heart has been observed already more than a century ago (Gaskell, 1882). ECG alternans has been connected to malignant arrhythmias and has become accepted as a predictor of forthcoming arrhythmic events (Rosenbaum et al., 1994). Consequently, numerous experiments and some numerical simulations investigating alternans have been carried out (Guevara et al., 1989; Lewis and Guevara, 1990; Vinet et al., 1990; Chialvo et al., 1990; Vinet and Roberge, 1994; Brandt et al., 1997; Hall et al., 1997; Yehia et al., 1999; Hall et al., 1999), for a review refer to Euler (1999).

Alternans has been shown to exist in single cells, in experiment as well as in theory (Guevara et al., 1989) (see Section 2). Single heart cells and fibers

* Corresponding author
E-mail address: chr@itb.biologie.hu-berlin.de (C. Zemlin).

0303-2647/02/$ - see front matter
PII: S0303-2647(02)00015-1

are the smallest units to exhibit alternans and understanding the development of alternans should be most feasible in them.

In the context of paced systems, alternans is also called a 2:2 rhythm, as two stimuli lead to two action potentials of different shape. Likewise, a rhythm in which only every other stimulus induces an action potential is called a 2:1 rhythm. We study in detail the development of 2:2 and 2:1 rhythms in the paced Beeler–Reuter (BR) model of myocardial tissue as the stimulation frequency is increased. Previous experimental studies have shown that the 1:1→2:2 transition exists in bullfrog tissue (Guevara et al., 1989) and chicken tissue (Hall et al., 1999). Model studies showed that the 1:1→2:2 transition occurs in the BR model (Jensen et al., 1984; Guevara et al., 1989), a cable of BR cells (Lewis and Guevara, 1990) and a sheet of cells of the more detailed Luo–Rudy model (Arce et al., 1977). Besides, transitions from 1:1 to other rhythms than alternans and further bifurcations have been described in several studies (Anderson et al., 1972; El-Sherif et al., 1977; Yehia et al., 1999).

We find and study hysteresis and bistability in the onset of alternans in the BR model. Then we quantify how blocking individual ionic currents can inhibit the development of alternans. Finally, we extend the BR model to include scalable calcium buffers and see how calcium buffers efficiency influences the onset of alternans.

2. The stimulated Beeler–Reuter model

Ionic cell models were invented by Hodgkin and Huxley in 1952. Since then, many new ionic currents have been found and studied, and heart cell models aiming at completeness have become very complex (Lou and Rudy, 1994; Courtemanche et al., 1998; Priebe and Beuckelmann, 1998). Because we are not interested in a precise reconstruction of all cell properties but in an understanding of the mechanisms that lead to alternans, we chose the simple BR model as a starting point (Beeler and Reuter, 1977). It is the simplest ionic model that accurately reproduces the action potential of myocardial tissue (see Fig. 1) and is widely used to model ventricular cells (Lewis and Guevara, 1990; Chay, 1996; Pumir and Krinsky, 1999).

We add a periodic extra current to the BR model to simulate periodic excitation. Then we study the effect of increasing stimulation frequency.

2.1. The model equations

In the BR model (Beeler and Reuter, 1977), the transmembrane voltage V (always in mV) changes according to

$$\frac{dV}{dt} = -\left(\frac{1}{C_m}\right)(I_{ion} + I_{stim}), \tag{1}$$

where C_m is the membrane capacitance (in μF); I_{ion} is the sum of the ionic currents (in μA) and I_{stim} is the stimulus current. The ionic current I_{ion} consists of

$$I_{ion} = I_{Na} + I_s + I_{K_1} + I_{x_1}. \tag{2}$$

The fast inward sodium current I_{Na} is given by

$$I_{Na} = (g_{Na}m^3hj + g_{NaC})(V - E_{Na}), \tag{3}$$

where, g_{Na} is the maximal sodium conductivity; g_{NaC}, the sodium leak conductivity; E_{Na}, the sodium equilibrium potential and m, h, and j are gating variables. Similarly, the slow inward current I_s is given by

$$I_s = g_s df(V - E_s), \tag{4}$$

where, g_s is the maximal calcium conductivity; E_s, the calcium equilibrium potential (Beeler and

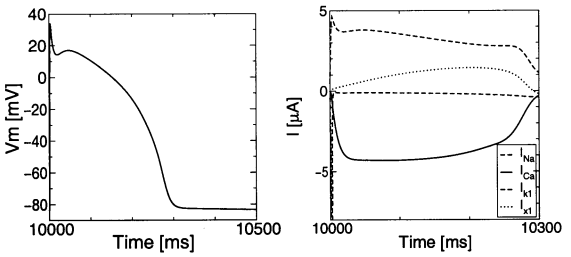

Fig. 1. Action potential (left) and ionic currents (right) in the BR model. Note that the sodium current is very short and very strong (it leaves the plotted range and goes down to −150 μA cm^{-2}).

Reuter, 1977) and d and f are gating variables. The potassium current I_{K_1} is simply a function of transmembrane voltage:

$$I_{K_1} = I_{K_1}(V), \tag{5}$$

and the time-activated outward current I_{x_1},

$$I_{x_1} = x_1 \bar{I}_{x_1}(V), \tag{6}$$

has a gating variable x_1. The functions I_{K_1} and I_{K_2} are given in Beeler and Reuter (1977). The gating variables m, h, j, d, f, and x_1 follow the dynamics

$$\frac{dy}{dt} = \left(\frac{y_\infty(V) - y}{\tau_y(V)}\right); \quad y \in \{m,\ h,\ j,\ d,\ f,\ x_1\}. \tag{7}$$

The individual expressions for in y_∞ and τ_y are given in Beeler and Reuter (1977). Finally, the intracellular calcium Ca_i, (always in μm) changes according to

$$\frac{d}{dt}\ Ca_i = -k_i I_s + \frac{1}{\tau_{Ca}}(Ca_{i,eq} - Ca_i), \tag{8}$$

where the second term on the right hand side implements a restoring force that drives intracellular calcium towards $Ca_{i,eq} = 0.1$ μM. For integration, we use a forward Euler scheme with $\Delta t =$ 0.02 ms.

2.2. Stimulation

The BR model has an attractive fixed point at $(V, Ca_i, x_1, m, h, j, d, f) = (-84.6, 0.178, 0.0056, 0.011, 0.99, 0.97, 0.0030, 1.00)$, corresponding to the rest state of heart tissue. Stimulation is simulated by means of a short extra current I_{stim}. The duration of this current is taken to be 2 ms, which is a typical value used in experiments (Elharrar et al., 1984; Guevara et al., 1989; Lewis and Guevara, 1990; Murphy et al., 1996), and the amplitude is set at two times the threshold value necessary to induce an action potential (this threshold was 26 μA).

We consider the model's response to a stimulus an action potential whenever the sum of the ionic currents is negative at the end of the stimulus, i.e. if there is further depolarization due to the cell's own dynamics. For every action potential, we define the action potential duration (APD) by the time between stimulus and the moment where transmembrane voltage goes back below −20 mV.

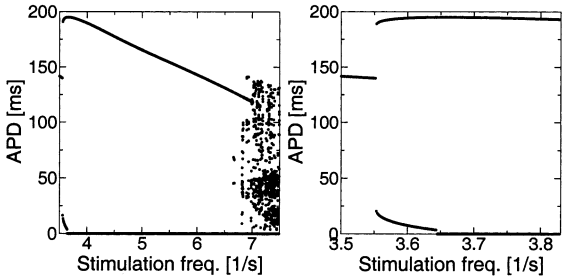

Fig. 2. Bifurcation diagram of the stimulated BR model. For every stimulation frequency we let 100 stimulations pass unrecorded and plot the following 20 APDs. Ineffective stimuli are assigned an APD of 0 ms. Right panel zooms into the first bifurcation, here we let 500 stimulations pass unrecorded.

To get an overview of the behavior at different stimulation frequencies, consider the sequence of APDs produced by stimulation at a certain frequency as plotted in Fig. 2. Alternans sets in at a frequency of about 3.55 s^{-1}. The duration of the shorter action potential drops quickly to below 50 ms and continues to decline. At 3.63 s^{-1}, there is a transition 2:2 → 2:1. This remains stable for a wide range of stimulation frequencies, and only at about 6.65 s^{-1} there are further bifurcations and irregular behavior, in good agreement with experimental results (Hescheler and Speicher, 1989). Note that we restarted the system from rest state for every frequency. The result is significantly different if the system is not restarted, as shown below.

3. 2:1 Development in the BR model

Fig. 3 shows in detail how a 2:1 rhythm sets in. It appears that the first signs of the transition are in the closing variable j of the sodium current. A simple explanation for the onset of 2:1 at high frequencies is that ever faster stimulation leaves less and less time for recovery, and at some point, j is no more reset to 1. In this situation, a newly given stimulus cannot initiate a sodium current, and the resulting voltage signal is much smaller than in a full action potential. In the following period, there is plenty of time for relaxation; thus,

the next stimulus can easily initiate a full action potential. The result is an alternation between full action potentials and small/no action potentials.

However, this explanation is somewhat simplistic. While it is true that alternation can be inhibited by letting j and h relax at higher voltages, one can inhibit 2:1 rhythms and alternans even better by changing other model features, as will be shown in Section 3.2.

3.1. Hysteresis and bistability

There is hysteresis in the onset of 2:1 in the BR model (see Fig. 4). We first increase the stimulation frequency in steps of 0.01 s^{-1}, this time without resetting the variables to rest state at each new frequency. Alternans sets in not before 3.7 s^{-1} and soon afterwards develops into a 2:1 rhythm. For decreasing stimulation frequency, a 2:1 rhythm persists down to 3.63 s^{-1}, followed by alternans down to 3.55 s^{-1}, where it is replaced by a 1:1 rhythm. Hysteresis has been reported recently in the Luo–Rudy model (Yehia et al., 1999) as well. Thus, in any study of alternans onset, the initial conditions have to be specified.

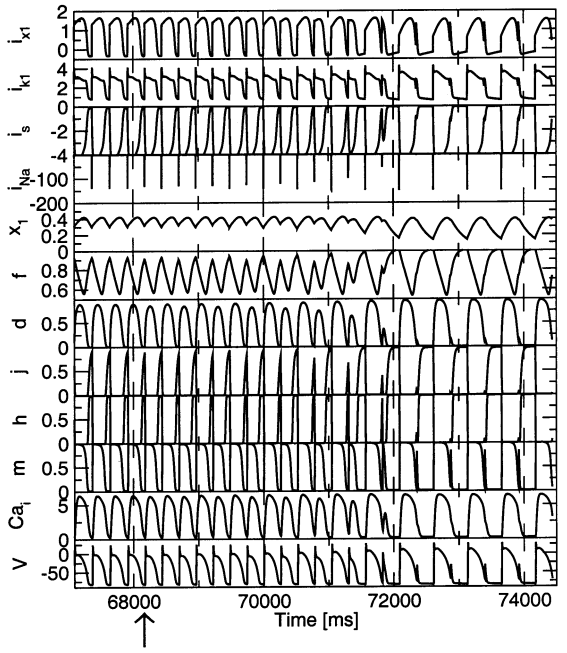

Fig. 3. All model variables and ionic currents as a 2:1 rhythm sets in. Stimulation frequency has been increased in steps of 0.01 s^{-1} without initializing, so that 2:1 has not yet set in at 3.67 s^{-1}. We show the last four stimulations at 3.67 s^{-1} and then switch to 3.83 s^{-1} stimulation (arrow), again without initializing. After some transients, there is a stable 2:1 rhythm. Units are mV for V, μM for Ca_i and μA for the currents.

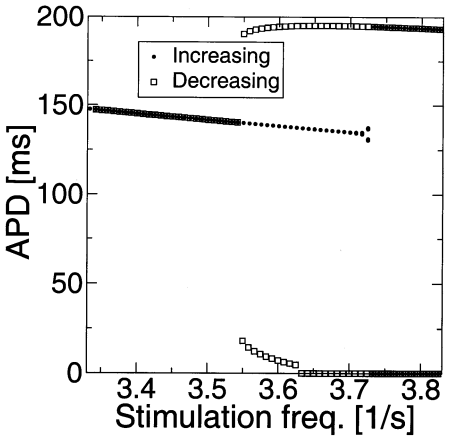

Fig. 4. Hysteresis in the onset of alternans. Solid circles show the onset of alternans for increasing frequency, empty squares for decreasing frequency. We changed stimulation frequency in steps of 0.01 s^{-1}, using the final state of one frequency as the initial state of the next.

The presence of hysteresis shows that, at certain frequencies, there are at least two attractors in phase space, the 1:1 attractor and the 2:2/2:1 attractor. The 1:1 attractor disappears for sufficiently high frequencies, whereas the 2:2/2:1 attractor disappears for sufficiently low frequencies. To understand this effect in more detail, we study the development of the basins of these two attractors with changing frequency. As the system is eight-dimensional, a complete determination of the basins is impractical, so we take two different approaches.

In our first study, we consider not full phase space but a physiologically especially important subset, i.e. the set of states traversed during a standard action potential (from 1 s^{-1} stimulation). This subset can be parameterized by the phase of the action potential, which we normalize to range from 0 to 1. Our question thus becomes which phases of the standard 1 s^{-1} action potential as initial condition lead to a 1:1 rhythm and which to a 2:2/2:1 rhythm; this depends on stimulation frequency. Fig. 5 shows the results. As expected,

the basin of the 1:1 attractor becomes progressively smaller with frequency. A phase close to one drops out of the 1:1 attractor already at a rather low frequency. This is because the first stimulation will produce a long action potential and the second stimulation is likely to meet un-recovered tissue; this is a good starting point for alternans. Note that stimulation from rest state leads to alternans easily for the same reason. Indeed, the bifurcation frequency in Fig. 2 almost coincides with the frequency at which the 1:1 basin starts getting smaller (ca. 3.55 s^{-1} in both cases), and also with the frequency of the 2:2→1:1 transition in Fig. 4. On the other hand, in two small intervals of initial phases around 0.07 and 0.343, the 1:1 rhythm is stable almost as long as in the hysteresis protocol. This shows that our chosen subset gets close (in phase space) to the 1:1 attractor over the whole range of frequencies considered.

In a second study, we studied how results of our original hysteresis protocol change if we add uncorrelated equally distributed noise to the transmembrane voltage in every time step. This is a way of testing how close to the boundary of the basin the system is as it moves along the attractor.

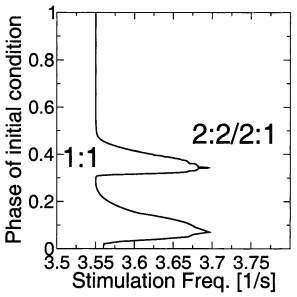

Fig. 5. Basins of the 1:1 and the 2:2/2:1 attractor as a function of stimulation frequency. We consider as initial conditions states from a standard 1 s^{-1}-stimulation limit cycle (parameterized by its phase). Each vertical section of the figure shows which of these initial conditions lead to 1:1 and which to a 2:1/2:2 rhythm. Reading the figure from left to right, for low frequencies, any initial condition from the standard cycle leads to a 1:1 rhythm, while for faster stimulation, an ever smaller part does so; for frequencies above 3.7 s^{-1}, any initial condition from the standard cycle leads to a 2:2/2:1 rhythm. For phases between 0 and 0.15, V reaches values outside our tabulation range, so for these phases, we performed calculation without tabulation. For a given phase, the alternans onset frequency rises by about 0.01 s^{-1} if tabulation is turned off.

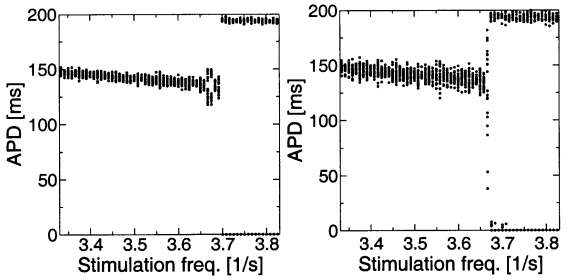

Fig. 6. The effect of noise on the stability of rhythms. The protocol is as in Fig. 4, but at each time step, we add uncorrelated equally distributed noise to V. In the left panel, the amplitude of this noise is ±2 mV, in the right panel ±4 mV.

Fig. 6 shows that the increasing noise shifts the transition 1:1→2:1 to lower frequencies. In much the same way, increasing noise shifts the backward transition 2:2→1:1 to higher frequencies (no picture shown), but the shift is much smaller. This indicates that the basin of 2:2 disappears much more abruptly.

Finally, we use the insight we gained to demonstrate how accurately placed extra stimuli can induce switching from one attractor to the other in the bistable regime. In Fig. 7, the cell is paced at 3.56 s^{-1} and is initially in a 2:2 rhythm. By putting an extra stimulus at phase 0.5, we induce a switch to a 1:1 rhythm. After eight beats in 1:1 rhythm, we set another stimulus at phase 0.8. This induces a switch back to the 2:2 rhythm. The placement of both stimuli is not critical, the switching occurs for a range of phases.

3.2. Alternans inhibition

To inhibit alternans while retaining the basic action potential shape, either the relaxation has to be accelerated or the rest state has to be moved so

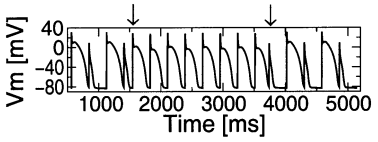

Fig. 7. In the bi-stable regime, a single well-timed pulse can switch rhythms. Starting from a 2:2 rhythm, an extra stimulus indicated by the first arrow induces a transition to a 1:1 rhythm. This transition is reversed by a second extra stimulus indicated by a second arrow.

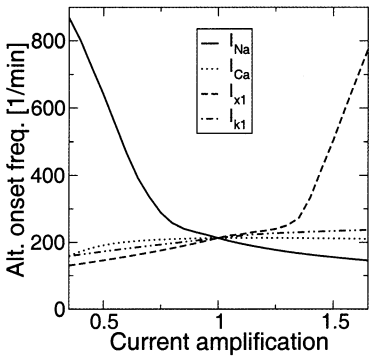

Fig. 8. Effect of modifying the ionic currents in the BR model on the development of altenans. For each ionic current, we introduced a global modification factor. We changed this modification factor from 0.35 to 2.0, where a, factor of 1 corresponds to the original current.

that it is reached earlier. Acceleration of the relaxation via modification of ionic currents is promising, because drugs to modify the channel behavior are known (Elharrar et al., 1984; Singh, 1999). We quantify the effect of altering an ionic current by introducing a constant c_{mod} by which the current is multiplied. For several values of c_{mod}, we determine the frequency of alternans onset. Note that this setting is also a valid description of natural deviations of current amplitudes, e.g. due to genetically caused differences in ion channel densities.

Fig. 8 shows the effect of modifying the sodium, calcium, and potassium currents.

Amplification of the sodium current inhibits alternans, because a strong initial peak in the action potential lifts x_1 so that repolarization is strong from the beginning. A stronger repolarizing potassium current also shifts the alternans onset frequency to higher values. A strong calcium current promotes alternans, because calcium is the main depolarizing current.

The onset of alternans is most sensitive to changes in the calcium current and the potassium current i_{K_1}. It is rather insensitive to i_{Na}, because no matter by which factor i_{Na} is multiplied, it is turned off by h soon after V becomes positive. The dependency on i_{x_1} is not strong either, because i_{x_1} is 'self-inhibiting'. A strong i_{x_1} inhibits excitation and that way prevents x_1 from becoming large at the initial peak. As a consequence, i_{x_1} does not grow as much as might be expected from the increase in x_1.

Moving the recovery threshold to higher transmembrane potentials obviously inhibits alternans, but the inhibition is significant only if the threshold is moved strongly (not shown).

4. Alternans and calcium buffering

Another mechanism in heart cells that might be effective in the development of alternans is calcium buffering. We will introduce simple calcium buffers with adjustable efficiency and study how the efficiency influences the onset of alternans. An overview of recent calcium buffer models can be found in Goldbeter (1996).

In the BR model, there is a 'restoring force' that drives $\mathrm{Ca_i}$ towards its resting value Eq. (8). This restoring force does not reflect calcium buffering adequately. In fact, the most important effect of the restoring force is that it drives the calcium back out of the cell, as there is no other outward calcium current. Therefore, when we introduce more realistic calcium buffering, we cannot just drop the restoring force, and we will keep it with the calcium buffers we introduce. We interpret the restoring force as an outward calcium current that serves to maintain equilibrium calcium concentration.

The structure in the cell that stores calcium is the sarcoplasmic reticulum (SR), a network of tubes that pervades the cell. Parts of the surface of the SR contain pumps that transport calcium from the myoplasm into the SR; the corresponding parts of the SR are called *uptake* compartments. In other parts of the SR, ion channels for calcium release dominate, they are called the release compartments. This structure suggests two-compartment calcium buffers, which are in fact used in detailed modeling of calcium dynamics (Lou and Rudy, 1994). The compartments and calcium currents between them are shown in Fig. 9. The dynamic equations are:

$$\frac{\mathrm{d}}{\mathrm{d}t}\,\mathrm{Ca_i} = j_3 - j_1$$

$$\frac{\mathrm{d}}{\mathrm{d}t}\,\mathrm{Ca_u} = \frac{(j_1 - j_2)}{V_\mathrm{u}}$$

$$\frac{\mathrm{d}}{\mathrm{d}t}\,\mathrm{Ca_r} = \frac{(j_2 - j_3)}{V_\mathrm{r}}, \tag{9}$$

where, $\mathrm{Ca_i}$, $\mathrm{Ca_u}$ and $\mathrm{Ca_r}$ are the calcium concentrations (in μM) of the intracellular medium, the uptake, and the release compartment, respectively; V_u, the volume of the uptake compartment, and V_r is the volume of the release compartment, the volume of the myoplasm has been normalized to 1.

We chose the currents j_i in the simplest possible way compatible with physiology. The calcium uptake j_1 is caused by pumps, which are usually modeled using Michaelis–Menten kinetics. We further simplify j_1 by assuming linear operation, $j_\mathrm{I} = d_1\mathrm{Ca_i}$. The translocation of the calcium from uptake to release compartment is brought about by diffusion and modeled here (as usual) by $j_2 = d_2(\mathrm{Ca_u} - \mathrm{Ca_r})$ Calcium release j_3 increases with Ca_i as well as with $\mathrm{Ca_r}$ ('calcium-induced calcium release'). Physiologic models often use complicated formulations for this current. We chose the simplest term that includes the basic dependency on both $\mathrm{Ca_i}$ and $\mathrm{Ca_r}$, $j_3 = d_3\mathrm{Ca_i}\mathrm{Ca_r}$.

The resulting model still has the free parameters d_1, d_2 and d_3 (V_u and V_r are known (Lou and Rudy, 1994)). We think the best way to get realistic values for the free parameters is to impose conditions on important physiological quantities that can easily be measured and functionally depend on d_1, d_2, and d_3. We consider the steady state values of $\mathrm{Ca_i}$, $\mathrm{Ca_u}$, and $\mathrm{Ca_r}$ in the absence of calcium current from the extracellular medium, i.e. we disconnect the BR model from the calcium dynamics. Setting $j_1 = j_2 = j_3$ in Eq. (9) becomes:

$$d_1\mathrm{Ca_i} = d_2(\mathrm{Ca_u} - \mathrm{Ca_r}) = d_3\mathrm{Ca_i}\mathrm{Ca_r}. \tag{10}$$

Therefore,

$$\mathrm{Ca_r} = \frac{d_1}{d_3}, \quad \text{and} \quad \mathrm{Ca_u} = \frac{d_1}{d_3} + \frac{d_1}{d_2}\,\mathrm{Ca_i}. \tag{11}$$

Two conditions are imposed on d_1, d_2, and d_3 if $\mathrm{Ca_i}$, $\mathrm{Ca_u}$, and $\mathrm{Ca_r}$ are required to take on physiologically realistic values (the order of those given in Lou and Rudy, 1994), $\mathrm{Ca_i} \approx 0.17$ μM, $\mathrm{Ca_u} \approx 1800$ μM, and $\mathrm{Ca_r} \approx 1800$ μM). We use the last free parameter for the adjustment of the time constant τ with which perturbations of the steady state relax. The functional dependency of τ on d_1, d_2 and d_3 is gained by linearizing the dynamics (Eq. (9)) at the steady state and calculating the eigenvalues of the Jacobi matrix. Setting $\tau = 180$ ms, a typical time-constant of Ca-relaxation (Lou and Rudy, 1994), yields after some calculation.

$$d_1 = 8.67 \times 10^{-2}, \quad d_2 = 1.56 \times 10^{-4}, \quad d_3 = 50.98. \tag{12}$$

We now consider the model as shown in Fig. 9. The BR equations and the calcium buffer equations are linked at the intracellular calcium, whose rate of change is:

$$\frac{\mathrm{d}}{\mathrm{d}t}\,\mathrm{Ca_i} = -k_i I_\mathrm{s} + \frac{1}{\tau_\mathrm{Ca}}(\mathrm{Ca_{i,eq}} - \mathrm{Ca_i}) - d_1\mathrm{Ca_i} + d_3\mathrm{Ca_r}\mathrm{Ca_i}. \tag{13}$$

The basic structure of the bifurcation diagram of the BR model is not changed by the new Ca-buffering mechanism (Fig. 10).

To assess the effect of calcium buffers quantitatively, we simultaneously vary the strength j_1 and j_3 by multiplying them with an identical factor and determine the corresponding alternans onset frequencies. As shown in Fig. 10, the stronger the

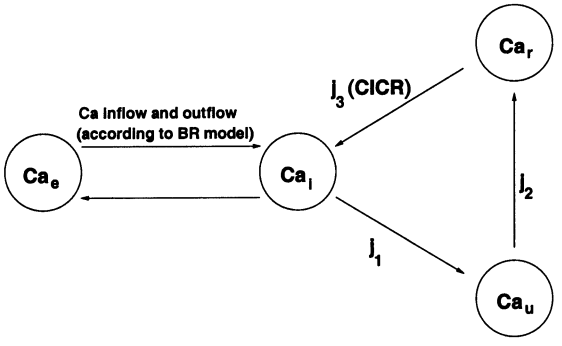

Fig. 9. Structure of the proposed model for calcium buffers in the cell. The $\mathrm{Ca_e}$ compartment represents the extracellular medium, the $\mathrm{Ca_i}$ compartment the myoplasm and the $\mathrm{Ca_u}$ and $\mathrm{Ca_r}$ compartments the calcium uptake and release parts of the sarcoplasmic recticulum.

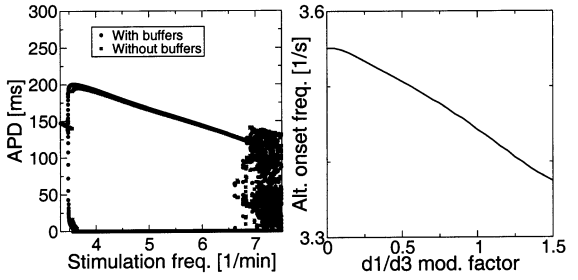

Fig. 10. The effect of the calcium buffers on the onset of alternans. Left panel shows the slight shift towards lower frequencies in the bifurcation diagram. The protocol is as in Fig. 2. Right panel shows the shift of alternans onset frequency as a function of calcium buffer efficiency; here we restarted from rest state for each frequency.

uptake pump, the earlier alternans sets in, which means that calcium buffering promotes the development of alternans.

To understand this effect, consider how the net calcium inflow $\mathrm{d}/\mathrm{d}t(\mathrm{Ca_i})$ is modified by the buffers. The effect of the calcium buffers has two components, which can clearly be seen in Fig. 11. On the one hand the calcium release, which is fast but small, produces an extra initial peak in $\mathrm{Ca_i}$. On the other hand, the calcium uptake considerably decreases $\mathrm{Ca_i}$ over the second part of the action potential. The lower $\mathrm{Ca_i}$ causes the equilibrium potential for calcium to rise and that way increases the calcium current slightly Eq. (4). As the calcium current is depolarizing, repolarization is delayed. The balance of de- and repolarizing currents during an action potential is delicate, so that the slight change in calcium current leads to a sizable shift of alternans onset frequency.

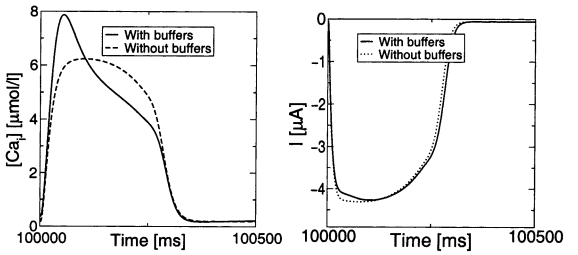

Fig. 11. The effect of the calcium buffers on calcium concentration and calcium current. In both panels, model cells were stimulated at low frequency (1 $\mathrm{s^{-1}}$) and transient have passed.

5. Discussion

Alternans is linked to dangerous arrhythmias and understanding its mechanisms is of great clinical importance. We studied the onset of alternans in a simple model. In this simple model, we were able to understand hysteresis and bistability at the onset of alternans, the potential for inhibiting alternans by blocking specific currents, and the influence of calcium buffers on alternans development. We believe that similar mechanisms apply to more detailed models and the real cell, where the existence of hysteresis and bistability has already been shown (Hall et al., 1999; Yehia et al., 1999).

We are not aware of any experimental study that investigates the effect of calcium buffers on alternans genesis. Methods for blocking of calcium buffers are, however, available (Asano and Nomura, 2000; Kabbara and Stephenson, 1997), so it can be tested if the mechanisms we describe are indeed effective, or if the relationship between calcium buffering and alternans genesis is more complex in real cells.

Appendix A: Full list of modifications in the calcium buffer model

New state variables

$\mathrm{Ca_u}$ (μM)	calcium concentration in the uptake compartment
$\mathrm{Ca_r}$ (μM)	calcium concentration in the release compartment

New dynamic equations

$$\frac{\mathrm{d}}{\mathrm{d}t}\,\mathrm{Ca_i} = -0.1 i_{\mathrm{Ca}} + 0.07(0.1 - \mathrm{Ca_i}) - j_1 + j_3$$

$$\frac{\mathrm{d}}{\mathrm{d}t}\,\mathrm{Ca_u} = \frac{(j_1 - j_2)}{V_{\mathrm{u}}}$$

$$\frac{\mathrm{d}}{\mathrm{d}t}\,\mathrm{Ca_r} = \frac{(j_2 - j_3)}{V_{\mathrm{r}}} \qquad \text{(A.1)}$$

Calcium currents in the cell

$$j_1 = d_1 \mathrm{Ca_i}$$

$$j_2 = d_2(\mathrm{Ca_u} - \mathrm{Ca_r})$$

$$j_3 = d_3 \mathrm{Ca_i} \mathrm{Ca_r}, \qquad \text{(A.2)}$$

New constants

Name	Meaning	Value	Unit
d_1	strength of calcium uptake pump	0.0867	s^{-1}
d_2	strength of diffusion from uptake to release	1.56×10^{-4}	s^{-1}
d_3	strength of calcium-induced calcium release	50.98	s^{-1}
V_u	volume of the calcium buffer uptake compartment (relative to the cytoplasm volume)	0.06	
V_r	volume of the calcium buffer release compartment (relative to the cytoplasm volume)	0.006	

References

Anderson, G.J., Greenspan, K., Fisch, C., 1972. Electrophysiologic studies on Wenckebach structures below the atrioventricular junction. Am. J. Cardiol. 30, 232.

Arce, H., Xu, A., Gonzales, H., Guevara, M., 1977. Alternans and higher-order rhythms in an ionic model of a sheet of ischemic ventricular muscle. Chaos 268, 411–426.

Asano, M., Nomura, Y., 2000. Ca^{2+} movement from leaky sarcoplasmic recticulum during contraction of rat arterial smooth muscle. Eur. J. Pharmacol. 404, 327–329.

Beeler, G.W., Reuter, H., 1977. Reconstruction of the action potential of ventricular myocardial fibres. J. Physiol. (London) 268, 177–210.

Brandt, M.E., Shih, H., Chen, G., 1997. Linear time-delay feedback control of a pathological rhythm in a cardiac conduction model. Phys. Rev. E 56 (2), R1334–R1337.

Chay, R., 1996. Proarrhythmic and antiarrythmic actions of ion channel blockers on arrhythmias in the heart: model study. Am. J. Physiol. 271, 329–356.

Chialvo, D.R., Gilmour, R.F., Jalife, J., 1990. Low dimensional chaos in cardiac tissue. Nature 343, 653–656.

Courtemanche, M., Ramirez, R.J., Nattel, S., 1998. Ionic mechanisms underlying human atrial potential properties: insights from a mathematical model. Am. J. Physiol. 275, H301–H321.

El-Sherif, R., Hope, R.R., Scherlag, B.J., Lazara, R., 1977. Reentrant ventricular arrhythmias in the late myocardial infarction period. Circulation 55, 702–718.

Elharrar, V., Atarashi, H., Surawicz, B., 1984. Cycle length-dependent action potential duration in canine cardiac purkinje fibers. Am. J. Physiol. 247 (6 Pt3), H936–H955.

Euler, D.E., 1999. Cardiac alternanns: mechanisms and pathophysiological significance. Cardiovasc. Res. 42, 583–590.

Gaskell, W.H., 1882. On the rhythm of the heart of the frog, and on the nature of the action of the vagus nerve. Phil. Trans. R. Soc. London 173, 993–1033.

Glass, L., Mackey, M., 1988. From Clocks to Chaos. Princeton University Press, Princeton.

Glass, L., Hunter, P., McCulloch, A. (Eds.), Theory of Heart. Springer, New York 1991.

Goldbeter, A., 1996. Biochemical Oscillations and Cellular Rhythms. Cambridge University Press, Cambridge.

Guevara, M.R., Alonso, F., Jeandupeux, D., van Ginneken, A.C.G., 1989. Alternans in periodically stimulated isolated ventricular myocytes: experiment and model. In: Cell to Cell Signalling: from Experiment to Theoretical Models. Academic Press, London, pp. 551–563.

Hall, K., Christini, D.J., Tremblay, M., Collins, J.J., Glass, L., Billette, J., 1997. Dynamic control of cardiac alternans. Phys. Rev. Lett. 78, 4518–4520.

Hall, G.M., Bahar, S., Gauthier, J., 1999. Prevalence of rate-dependent bevaviours in cardiac muscle. Phys. Rev. Lett. 82 (14), 2995–2998.

Hescheler, J., Speicher, R., 1989. Regular and chaotic behaviour of cardiac cells stimulated at frequencies between 2 and 20 Hz. Eur. Biophys. J. 17, 273–280.

Jensen, J.H., Christiansen, P.L., Scott, A.C., 1984. Chaos in the Beeler–Reuter system for the action potential of ventricular myocardial fibers. Physica D 13, 269–277.

Kabbara, A.A., Stephenson, D.G., 1997. Ca^{2+} handling by rat myocardium exposed to ATP solutions of different $[Ca^{2+}]$ and Ca^{2+} buffering capacity. Am. J. Physiol. 273, H1347–1357.

Lewis, T.J., Guevara, M.R., 1990. Chaotic dynamics in an ionic model of the propagated cardiac action potential. J. Theor. Biol. 146, 407–432.

Lou, C.H., Rudy, Y., 1994. A dynamic model of the cardiac ventricular action potential I. Circ. Res. 74, 1071–1096.

Murphy, C.F., Horner, S.M., Dick, D.J., Coen, B., Lab, M.J., 1996. Electrical alternans and the onset of rate-

induced pulsus alternans during acute regional ischemia in the anaesthetised pig heart. Cardiovas. Res. 32, 138–147.

Panfilov, A.V., Holden, A.V. (Eds.), Computational Biology of the Heart. Wiley, Chichester 1997.

Priebe, L., Beuckelmann, D.J., 1998. Simulation study of cellular electric properties in heart failure. Circ. Res. 82, 1206–1223.

Pumir, A., Krinsky, V., 1999. Unpinning of a rotating wave in cardiac muscle by an electric field. J. Theor. Biol. 199, 311–319.

Rosenbaum, D.S., Jackson, L.E., Smith, J.M., Garan, H., Ruskin, J.N., Cohen, R.J., 1994. Electrical altenans and vulnerability to ventricular arrhythmias. New Engl. J. Med. 330, 235241.

Singh, B.N., 1999. Current antiarrhythmic drugs: an overview of mechanisms of action and potential clinical utility. J. Cardiovasc. Electrophysiol. 10, 283–301.

Vinet, A., Roberge, F.A., 1994. Excitability and repolarization in an ionic model of the cardiac cell membrane. J. Theor. Biol. 170 (2), 183–199.

Vinet, A., Chialvo, D.R., Michaelis, C., Jalife, J., 1990. Nonlinear dynamics of rate-dependent activation in models of cardiac cells. Circ. Res. 67, 1510–1524.

Winfree, A.T., 1987. When Time Breaks Down. Princeton University Press, Princeton, p. 1987.

Yehia, A.R., Jeandupeux, D., Alonso, F., Guevara, M.R., 1999. Hysteresis and bistability in the direct transition from 1:1 to 2:1 rhythm in periodically driven ventricular cells. Chaos 9, 916–931.